

Effect of different catalyst ratios on the ring-opening metathesis polymerization (ROMP) of dicyclopentadiene

Zehan Zhang¹, Zaixing Yang², Fei Zhou², Xuelian He^{1*}

¹Shanghai Key Laboratory of Multiphase Material Chemical Engineering, East China University of Science and Technology, Shanghai 200237, China

²Sinopec Shanghai Petrochemical Co., Ltd.

Received: 30 March 2022, Accepted: 21 May 2022

ABSTRACT

In this paper, the polymerization process of polydicyclopentadiene (PDCPD) obtained by using dicyclopentadiene (DCPD) and the 2nd generation Grubbs' catalyst is optimized. The curing reaction kinetics was studied by differential scanning calorimetry (DSC), and the solidification reaction process was obtained. The effects of different ratios of monomer to catalyst on the product performance were investigated. In addition, the current common modification methods of PDCPD have been summarized and improved. The results showed that with the increase of the ratio of monomer to the catalyst, the tensile strength, tensile modulus, bending strength and bending modulus of PDCPD all showed a downward trend, and the impact strength showed an upward trend. When nDCPD: nCat = 10000:1, the comprehensive mechanical properties of PDCPD reached the best. The bending modulus, tensile strength and impact strength of PDCPD achieved 2100 MPa, 52.4 MPa and 30 kJ/m², respectively. The glass transition temperature (T_g) of PDCPD also showed a decreasing trend with the increase of the ratio of monomer to the catalyst, at this ratio, the T_g of the polymer reached 147.6°C. The catalyst concentration had a large effect on the product performance. **Polyolefins J (2022) 9: 151-162**

Keywords: Polydicyclopentadiene, kinetics (polym.); catalyst concentration; reaction injection molding; ROMP.

INTRODUCTION

Polydicyclopentadiene (PDCPD) is obtained by the ring-opening metathesis polymerization (ROMP) of dicyclopentadiene (DCPD) monomer purified from C5 fraction [1]. PDCPD is widely used in the fields of auto parts, sports equipment and furniture shells due to its excellent mechanical and thermal properties. The downstream products of DCPD mainly include petroleum resin, unsaturated polyester resin, ethylene propylene

rubber and PDCPD, etc. Among them, DCPD petroleum resin can be used in various fields, such as ink paint and rubber adhesive. Unsaturated polyester resins can be significantly enhanced by DCPD modification to achieve their own hydrolytic stability [2]. As the third monomer besides ethylene and propylene, DCPD can also be used to synthesize ethylene propylene diene monomer (EPDM) rubber. Thus, a new polymer material

*Corresponding Author - E-mail: hexl@ecust.edu.cn

PDCPD was prepared by reaction injection molding (RIM) method in the 1990s [3]. The process has the advantages of low cost, fast forming, short production cycle, convenience and high efficiency, so it can be used to prepare a variety of forming sheets [4-6].

PDCPD is mainly machined via reaction injection molding (RIM), resin transfer molding (RTM) and vacuum-assisted RTM (VARTM) [7-11]. At present, industrial factories mainly use RIM to produce PDCPD sheets based on lower viscosity and faster polymerization speed of DCPD [12,13]. This reaction procedure will result in the development of cross-linked PDCPD (Figure 1). Related studies [14] have shown that as the reaction continues, cyclopentene rings in DCPD will also open, and they will combine with the double bonds on the main chain, and then cross-linking reaction occurs, and finally a highly cross-linked PDCPD is formed. As current PDCPD technology is not proficient enough, raw material purification technology and mold process design are restricted, resulting in high application costs and low market awareness. This paper aims to find the best PDCPD synthesis process, optimize the RIM process, and reduce the loss of the reaction process [14,15].

Ruthenium metal Grubbs' catalysts are known to be highly active and stable, and are highly tolerant to olefins bearing functional groups, water and air [16-18]. In the early 1990s, Schrock et al. [19-22] synthesized a molybdenum carbene complex with Mo as the metal active center, known as Schrock catalyst. However, the poor functional group tolerance and sensitivity to

protic solvents and air of Schrock catalysts have limited real breakthroughs in this field. In view of the fatal shortcomings of Schrock catalysts that are not resistant to water and oxygen [23], Grubbs and his research group have successfully synthesized a carbene complex with ruthenium as the metal active center [24,25], which is the 1st generation Grubbs' catalyst. In the late 1990s, Grubbs et al. continued to carry out a series of experiments and studies, and found that the metal carbene structure was formed by dissociation of phosphine ligands during the ROMP reaction. Therefore, Grubbs et al. tried to replace the cyclohexylphosphine ligand (PCy₃) with a nitrogen heterocycle (H₂IMes) [26,27] to obtain the 2nd generation Grubbs' catalyst (Figure 2). Compared to the 1st generation Grubbs' catalysts, the 2nd generation Grubbs' catalysts are less sensitive to water and oxygen. At the same time, H₂IMes has stronger electron donating ability, so the catalytic activity of the 2nd generation catalyst is several magnitudes higher than that of the 1st generation catalyst. For the same monomer, a smaller amount of catalyst can be used to make the ROMP reaction of the monomer. Therefore, in this paper, the 2nd generation Grubbs' catalyst was used to initiate the reaction, and the most suitable molar ratio of monomer to catalyst was studied.

In recent years, the market of self-healing agents in the field of self-healing tends to use DCPD monomer with Grubbs' catalyst [28,29]. Kessler et al. [30] studied the curing kinetics of the DCPD/Grubbs' catalyst reaction system and found that different catalyst ratios had a great effect on the reaction kinetics. Yang et al. [31] investigated the reaction solidification kinetics of DCPD with refined 1st and 2nd generation Grubbs' catalysts and found that the 2nd generation catalyst system had higher reactivity and stability. Especially for thermoset materials, curing kinetics is the key to determining their

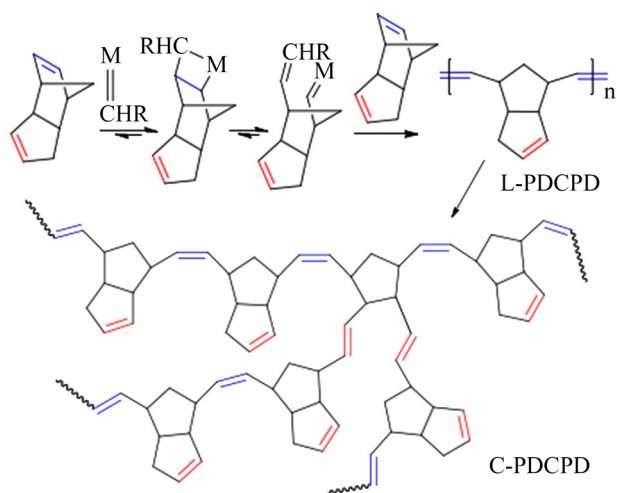


Figure 1. Mechanism for the ROMP of DCPD.

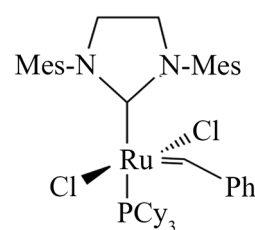


Figure 2. Structure of the 2nd generation Grubbs' catalyst.

reaction mechanism. The kinetic parameters of the reaction are usually measured by isothermal differential scanning calorimetry (DSC). However, there are two obvious drawbacks: firstly, the curing reaction may not be quite successful at lower temperatures, and on the other hand, the reaction may occur before the DSC reaches the required temperature. In addition, dynamic DSC data can provide more control over curing characteristics, and complex reaction mechanisms can be more easily explained by comparing measurements at different heating rates. In this study, dynamic DSC was used to analyze the curing kinetics of DCPD and 2nd Grubbs' generation catalyst at different ramp rates and catalyst concentrations.

In this paper, different proportions of DCPD monomer and 2nd Grubbs' generation catalyst were used for ROMP reaction, and the polymerization process of DCPD was studied and optimized. After that the curing process of DCPD was investigated by DSC, and the curing process was further determined. Finally, PDCPD was generated by the optimized RIM process. The effects of different monomer and catalyst ratios on the mechanical properties, reaction cure kinetics and thermodynamic properties of the products were analyzed.

EXPERIMENTAL

Materials

DCPD (95%) was purchased from Shanghai Bailingwei Chemical Technology Co., Ltd. China. The 2nd generation Grubbs' catalyst was procured from Shanghai Maikelin Chemical Technology Co., Ltd. China. Dichloromethane (CH₂Cl₂) was acquired from Shanghai Aladdin Biochemical Technology Co., Ltd., China.

Preparation of PDCPD

Polymerization of DCPD in Reagent Bottles

A Schlenk bottle was used to weigh 2 g of DCPD in a glove box, and 0.5 mL of dichloromethane solution was added to dissolve it. Then a certain amount of catalyst powder (the molar ratio of monomer to catalyst was 5000, 10000, 15000, 20000, 30000, 50000:1) was weighed in a sample bottle in the glove box, and 1 mL of dichloromethane solution was injected into it with a

syringe and shaken well to form a homogeneous catalyst solution. The catalyst solution was then added to DCPD for complete stirring, and the samples were removed after 1 h of reaction in a low-temperature bath at 20°C. In addition, the same steps were repeated at 20°C, 30°C, 35°C, 40°C and 60°C for several sets of experiments when the ratio of monomer to catalyst substance was controlled as 10000:1, and the gelation time was recorded with a stopwatch.

Preparation of PDCPD in Reaction Mold

A certain amount of DCPD was weighed in a Schlenk bottle and activated by heating in an oven, followed by the addition of dichloromethane for dissolution, and the mixed solution was placed in a low temperature reaction bath at 20°C and stirred well. A certain amount of catalyst powder (the molar ratio of monomer to catalyst was 5000, 10000, 15000, 20000, 30000, 50000:1) was weighed in the glove box and dissolved with CH₂Cl₂ (30mg/ml) solution, then the catalyst solution was pumped into the Schlenk bottle containing DCPD with a syringe, mixed and stirred thoroughly, and the dichloromethane solvent was pumped out until no air bubbles were produced. After that, the mixed solution was quickly injected into the reaction mold, which had been preheated to 60°C, and then sealed by passing nitrogen gas. After 1 h of reaction, the mold temperature was increased to 140°C and then cured for 1 h until the mold was cooled and the polymerized product was removed from the mold.

Conversion rate measurement

The samples prepared from the reagent bottles and the molded sheets prepared from the molds were mixed with the residual monomers and small molecule impurities that were not involved in the reaction. Therefore, the samples were placed in a vacuum drying oven at 80°C to remove these residual molecules, and then the conversion (CR) of the polymer product was obtained according to Equation 1.

$$CR = \frac{m_2}{m_1} \times 100\% \quad (1)$$

Where m_1 is the mass of the sample before vacuum drying and m_2 is the mass of the sample after vacuum drying.

Characterization

The samples were analyzed by infrared spectroscopy using a Fourier transform infrared (FTIR) spectrometer manufactured by Bruker, Germany, model VERTEX70. High-purity DCPD was solid at room temperature and all samples were prepared as pellets using spectroscopic grade KBr.

The thermal properties of the samples were determined on a DSC Q200 analyzer from TA, USA. The analysis was carried out under nitrogen atmosphere with ramping rates of 5°C/min, 8°C/min, 10°C/min and 15°C/min. The ramping range was 0-200°C. The monomer and catalyst were quickly mixed and placed in liquid nitrogen for flash freezing, and then 5-10 mg of the freezing solution or solid was put into the DSC aluminum tray and pressed for testing.

The swelling ratio (S) was obtained according to Equation 2, and the value of the crosslinking density V_e of each sample was obtained originally by the Flory formula:

$$S = \frac{m_2 - m_1}{m_1} \times 100\% \quad (2)$$

Thin slices with a thickness of 2 mm and a mass of about 100 mg were prepared and dried overnight in a vacuum drying oven at 60°C and weighed (m_1). The temperature in the drying oven was set at 30°C. A 100 mL brown wide-mouth bottle was taken and filled with a certain amount of toluene solvent, and the specimen was put into the wide-mouth bottle and then placed in the drying oven for about 4 days. At this time, the specimen began to swell, and when the swollen specimen reached saturation, meaning that the swelling reached equilibrium, the specimen was removed, dried on filter paper, and then weighed (m_2). Dynamic mechanical analysis (DMA) was carried out with a new thermomechanical analyzer DMA1 from Mettler-Toledo, Switzerland. The single cantilever mode was used, and the sample size was $35 \times 10 \times 4 \text{ mm}^3$. The loading frequency was 1 Hz, the heating rate was 3°C/min, and the heating range was 30°C-200°C.

Tensile, bending and impact strength tests were performed according to Chinese standards GB/T2567-2008. Tensile and bending samples were characterized by a CMT4204 microcomputer electronic universal testing machine from MTS, USA. Impact strength

was tested by a pendulum impact tester made by MTS, USA. All the data reported represented an average of the results on at least five specimens.

Thermogravimetric analysis (TGA) was performed on a Q500 dynamic thermomechanical analyzer from TA, USA. The samples were pre-dried in a vacuum drying oven, and about 10 mg of samples were weighed and tested under a nitrogen atmosphere, and the temperature was raised from 25°C to 600°C at 20°C/min.

RESULTS AND DISCUSSION

Polymerization process optimization

The effect of temperature

The effect of reaction temperature on the gel time and conversion of the polymerization reaction in a reagent bottle (monomer to catalyst molar ratio of 10000:1) is shown in Figure 3. With the increase of the reaction temperature, the gelation time of the polymerization reaction became shorter. At the temperature of 20°C, the gelation time was more than 25 min. But when the temperature was higher than 30°C, the reaction became very fast. Especially at 60°C, the reaction gelled within 2 min. In addition, after the DCPD reacted completely, the conversion rate of the polymer did not change very much with the change of temperature, and it was maintained at a relatively high level, all above 99%. Therefore, it was very important to choose the appropriate pretreatment temperature and reaction temperature for the polymerization reaction.

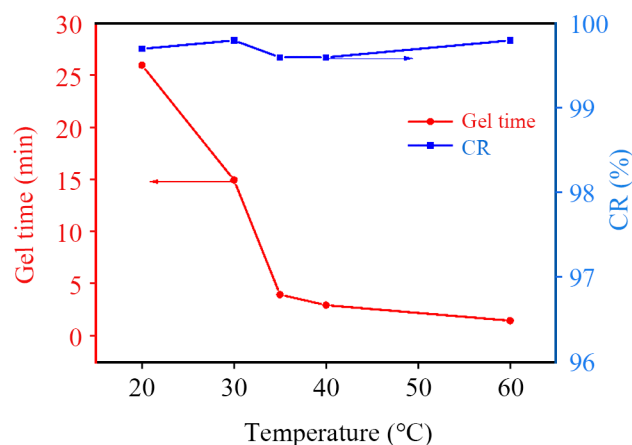


Figure 3. Effect of reaction temperature on gel time and conversion of polymerization.

Effect of monomer and catalyst ratio

Under the reaction condition of 20°C, the effect of different monomer and catalyst ratios in the reagent bottle on the gel time and conversion rate of the polymerization reaction is shown in Figure 4. It can be clearly seen from the figure that the gel time of the reaction was getting longer, and the gel time exceeded 25 min at 20°C, which was beneficial to the whole reaction pretreatment operation. In addition, the decrease of the catalyst content led to a lower number of reaction active centers, so the conversion rate of the reaction showed a downward trend. The relevant report [32] also confirmed this view. When the ratio of monomer to catalyst substance was less than 15000:1, the conversion rate of the whole reaction did not change much, and all of this was above 98%. After that, the conversion continued to decrease, so the ratio of monomer to catalyst should not be too large.

Structure of DCPD and PDCPD

In Figure 5, the IR spectra of DCPD and PDCPD are similar as a whole, but there are certain differences between 3100–2750 cm⁻¹ and 1700–1500 cm⁻¹. PDCPD has strong absorption peaks at 3050 cm⁻¹ and 1620 cm⁻¹, which are the stretching vibration peaks of =C-H and C=C in cyclic olefins, respectively. It showed that the PDCPD generated by DCPD still retains a large number of C=C structures (cyclopentene ring) after ring-opening metathesis polymerization.

As shown, the striking feature of linear PDCPD is the band at 3004 cm⁻¹. This absorption peak is the stretching vibration peak of the C-H bond in the acyclic

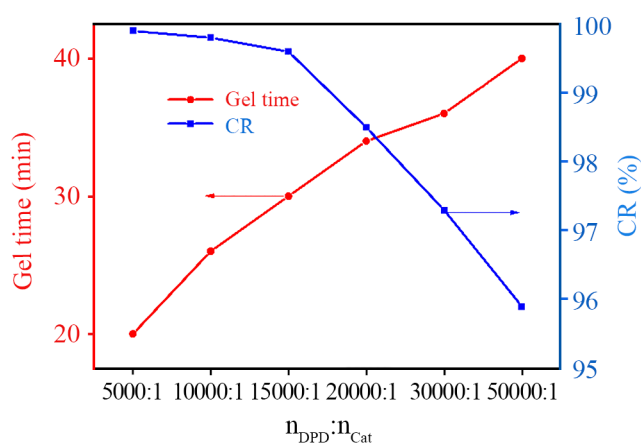


Figure 4. Effect of different monomer to catalyst ratios on gel time and conversion of polymerization.

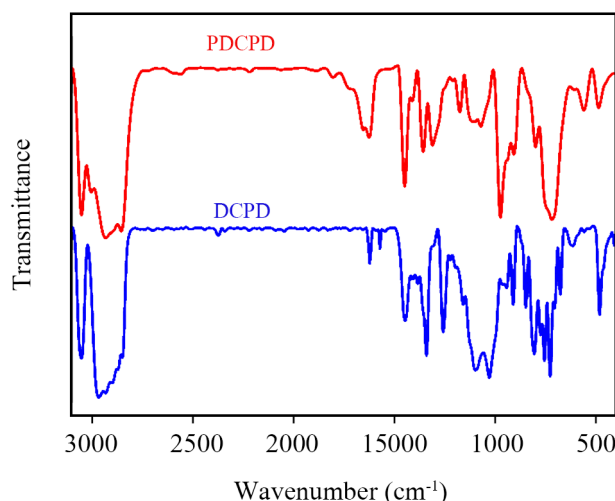


Figure 5. Infrared spectrum of DCPD and PDCPD.

olefin structure. In addition, 1571 cm⁻¹ is the absorption peak of C=C in the norbornene ring in DCPD, but there is no absorption peak in PDCPD, indicating that the norbornene ring in DCPD was opened, which completely verifies the speculative mechanism of ROMP. The relevant article [33] also supported this conclusion.

In the DCPD infrared spectrum, it could be seen that there were four absorption peaks at 2965 cm⁻¹, 2918 cm⁻¹, 2865 cm⁻¹, 2848 cm⁻¹, which are the stretching vibration peaks of -CH₂ on the norbornene ring and on the cyclopentene ring. Compared with DCPD, the absorption peaks at 2965 cm⁻¹ and 2865 cm⁻¹ in PDCPD disappeared due to the opening of the norbornene ring, resulting in a smaller -CH₂ tension and overlapping with -CH₂ in the cyclopentene ring, which also indirectly verified the ROMP mechanism.

Curing reaction kinetics

DSC curing process

The extraction of DSC reaction curve data can be used to study the crosslinking reaction kinetics of DCPD (including surface activation energy (*E_a*) and reaction order (*n*)). The same DSC analysis was performed on samples at different monomer to catalyst ratios. Figure 6 shows the dynamic DSC scans of DCPD with the DCPD monomer to catalyst substance ratios of 10000:1 and 15000:1 at different heating rates. The peak shapes and trends of these two DSC curves are very similar, and the ratio of 10000:1 was used as an example to analyze the curing reaction. In the curve,

there is an endothermic peak between 0°C and 35°C, and the corresponding temperature is the melting point of DCPD, where the endothermic peak had little effect on the enthalpy change of the entire curing reaction and could be ignored. A smoothing treatment was adopted to eliminate the influence of the melting phenomenon on the entire curing reaction curve. As the heating rate increased, the exothermic peak of the curing reaction in the DSC curve shifted to the right (high temperature), this was because when the heating rate was low, the curing reaction had enough time to proceed, but when the heating rate increased, the curing reaction would be delayed, resulting in the "thermal lag" phenomenon in the curve.

In Figure 6 (a), the initial temperature (T_i), peak top temperature (T_p), and peak termination temperature (T_f) of the sample in the reaction system at these four heating rates are obtained and listed in Table 1.

DSC data were not the characteristic temperature required for the curing process. Only when the heating rate was very small, the corresponding T_i , T_p , and T_f were the required curing temperatures. In this paper, the (T - β) extrapolation method was used to derive the characteristic temperature. The corresponding temperatures obtained for different rates in DSC were first fitted with a ($T=a\beta+b$) straight line to obtain Figure 7, and then extrapolated to get the rates. When it was 0, the converted temperature was the characteristic temperature. It could be seen from the figure that when $\beta = 0$, the T_i (gel temperature), T_p (curing temperature), and T_f (post-treatment temperature) of the DCPD curing reaction

Table 1. Reaction temperatures on the curing curves of DSC at different heating rates.

β (°C/min)	T_i (°C)	T_p (°C)	T_f (°C)	$1000/T_p$	$-\ln(\beta/T_p^2)$	$\ln \beta$
5	30.34	63.12	148.78	2.97	10.03	1.61
8	33.33	73.32	153.16	2.89	9.62	2.08
10	35.38	77.71	158.88	2.85	9.42	2.30
15	40.45	79.72	168.62	2.83	9.02	2.71

were 25.24°C, 58.54°C, and 138.07°C, respectively. In addition, this reaction system was a rapid prototyping process, but in order to obtain high-conversion polymer products, the reaction and post-curing time were both set as 1 h, and it was concluded that the curing process of PDCPD was 25°C (1 h) + 60°C (1 h) + 140°C (1 h). Since 25°C was close to room temperature, only 60°C (1 h) + 140°C (1 h) was needed to complete the reaction for saving time.

Curing reaction kinetic parameters

Some kinetic parameters, such as surface activation energy (E_a) and reaction order (n), were extracted from the DSC curve. According to Kissinger equation, curing reaction rate equation and Crane equation, the curing reaction activation energy and reaction order of the system were studied.

Kissinger [34] equation:

$$-\ln \frac{\beta}{T_p^2} = \frac{E_a}{RT_p} - \ln \frac{AR}{E_a} \quad (3)$$

Crane equation:

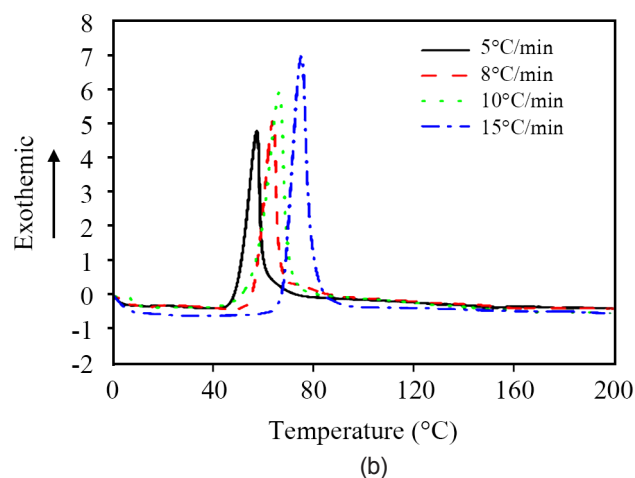
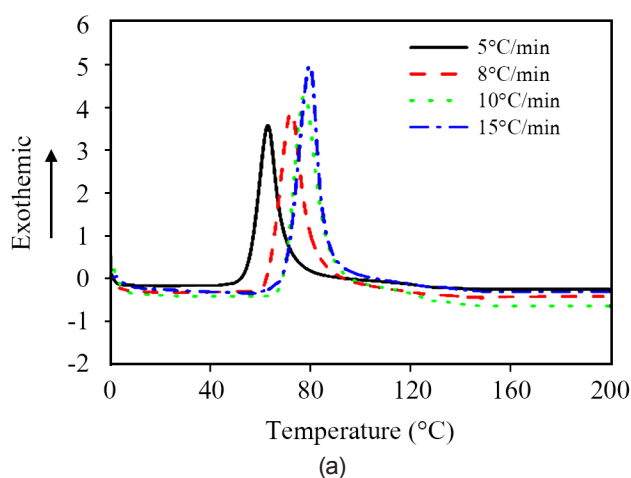


Figure 6. DSC curves for (a) the low-concentration (nDCPD:nCat=10000:1) and (b) the high-concentration (nDCPD:nCat=15000:1) of DCPD and Grubbs' catalyst samples.

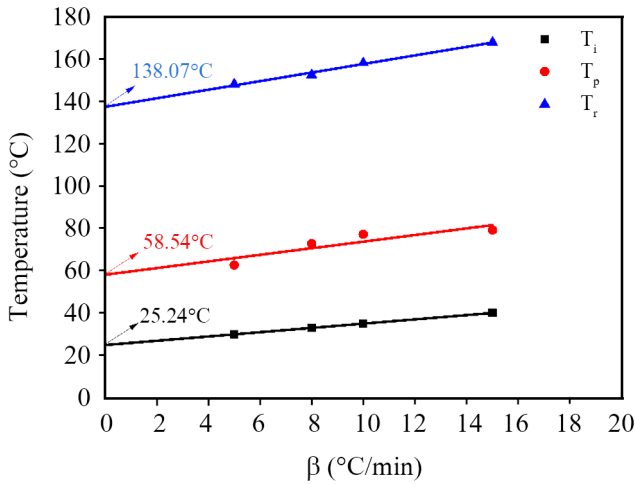


Figure 7. T- β linear fit extrapolated straight line for DCPD.

$$\frac{d \ln \beta}{d \frac{1}{T_p}} = -\frac{E_a}{nR} + 2T_p \quad (4)$$

For

$$\frac{E_a}{nR} \gg 2T_p \quad (5)$$

$$\frac{d \ln \beta}{d \frac{1}{T_p}} = -\frac{E_a}{nR} \quad (6)$$

Where the reaction rate constant is calculated using the following equation:

$$k = A e^{\frac{-E_a}{RT}} \quad (7)$$

Where the curing reaction rate equation is as follows:

$$\frac{d\alpha}{dt} = k(1-\alpha)^n \quad (8)$$

In these equations, α denotes the degree of cure, β (in K/s) is the heating rate, A (in s^{-1}) the pre-exponential factor, E_a (in J/mol) the activation energy, T_p (in K) the temperature, R (in J/mol K) the universal gas constant.

First, the two parameters $-\ln \frac{\beta}{T_p^2}$ and $\frac{1}{T_p}$ can be calculated from the peak top temperature and the corresponding heating rate listed in Table 2, and then subjected to linear regression. The apparent activation energy of the reaction could be calculated from the slope of the fitted curve shown in Figure 8. Specifically, the slope of the fitted straight line is 6.31, so the

activation energy (E_a) was obtained as 52.5 kJ/mol. The intercept of the fitted line on the y-axis is -9.15, so the pre-exponential (A) was obtained as 5.94×10^7 .

According to $-\ln \frac{\beta}{T_p^2}$ and $\frac{1}{T_p}$, a straight line fitting graph can be drawn, and the slope of the straight line can be achieved 6.98, so the reaction order (n) was obtained as 0.904. Therefore, the curing reaction rate equation of DCPD is:

$$\frac{d\alpha}{dt} = 5.94 \times 10^7 e^{\frac{-6309.8}{T}} (1-\alpha)^{0.904} \quad (9)$$

Effect of Monomer to Catalyst Ratio on Kinetic Parameters

The surface activation energy (E_a) and reaction order (n) of different monomer to catalyst ratios are shown in Table 2. It is clear that the ratio of monomer to catalyst is proportional to the magnitude of the activation energy. This is because the decreased catalyst content leads to fewer activation centers, which results in higher energy barriers to be overcome and activity of the polymerization reaction.

Swelling degree

The swelling ratio was used to reflect the crosslink density of all polymers. The swelling ratios of PDCPD prepared with different monomer to catalyst ratios are shown in Table 2. The swelling ratio and the crosslinking density showed an opposite trend, the larger the swelling ratio, the smaller the crosslinking density. It could be attributed that the number of catalysts determines the number of reactive centers. When the catalyst content was reduced, the number of reactive centers was relatively small, and the degree of crosslinking reaction of DCPD was not enough. In fact, when the ratio of monomer to catalyst substance was 10000:1, the change in crosslink density was relatively gentle, and the change was not great compared with the polymer prepared when the molar ratio was

Table 2. Surface activation energy, reaction series and swelling degree at different ratios.

$n_{\text{DCPD}}:n_{\text{Cat}}$	E_a (kJ/mol)	n	Swelling degree (%)
5000:1	52.5	0.902	61.3
10000:1	53.7	0.922	63.3
15000:1	54.0	0.930	64.1
20000:1	54.8	0.935	101.6
30000:1	54.9	0.946	105.2
50000:1	55.3	0.953	106.8

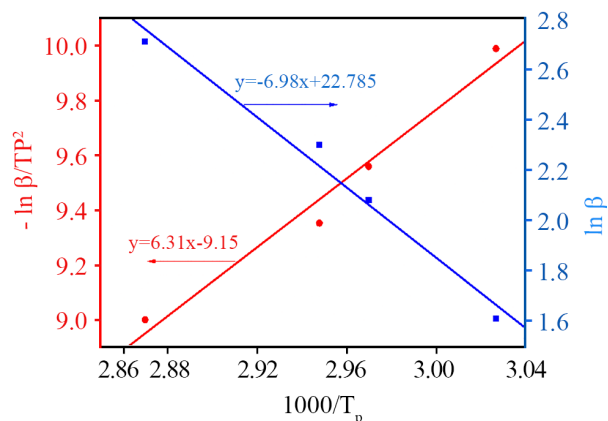


Figure 8. Linear fit graph of $-\ln \frac{\beta}{T_p^2}$ versus $\frac{1}{T_p}$ and $\ln \beta$ versus $\frac{1}{T_p}$.

5000:1. However, as the ratio of monomer to catalyst exceeded 10000:1, the swelling degree changed rapidly. Therefore, it was necessary to find a moderate molar ratio to ensure that there was a polymer with a suitable crosslinking density.

Dynamic mechanics

Figure 9 shows the relationship between the storage modulus (E') and loss factor ($\tan \delta$) of poly(DCPD) under different monomer to catalyst ratios with respect to temperature. The storage modulus in the glassy state (E' at 30°C) and the rubbery state (E' at $T_g + 30^\circ\text{C}$) were extracted from the E' -T curve in Figure 9(a). In addition, approximate crosslinking density (V_c) was calculated according to the rubber theory. The temperature corresponding to the peak point of the loss factor ($\tan \delta$)

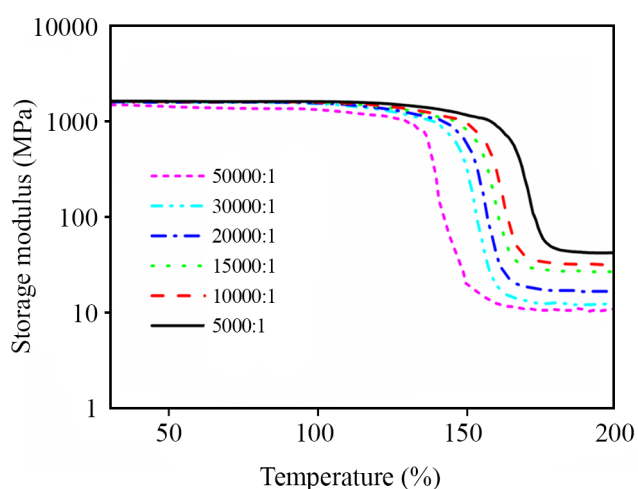


Figure 9. DMA curves of PDCPD: (a) Storage modulus (E'), (b) Loss factor ($\tan \delta$).

as a function of temperature was defined as the glass transition temperature (T_g), and this temperature was extracted from Figure 9(b). Finally, all the data were listed in Table 3.

With decreasing catalyst content, the storage moduli of all PDCPD samples in the glassy state at 30°C and in the rubbery state at $T_g + 30^\circ\text{C}$ showed a downward trend because of the amount of catalyst participation, the number of reactive sites and the reduction in polymer crosslink density (Table 3). The T_g of the polymer reflected the relaxation phenomenon that the chain segments began to move, and the T_g also decreased with the increment of the ratio of DCPD to catalyst. It could be reasonably inferred that as the crosslink density changed, the mobility of the chain segments became better, which was manifested by lower T_g . When the ratio of monomer to catalyst substance was 5000:1, the T_g was 151.78°C; when the ratio was higher than 10000:1, the T_g decreased rapidly; when the ratio was 50000:1, the T_g was as low as 112.3°C, indicating that the ratio of monomer to catalyst had a great influence on the thermal properties of the polymer. In order for the polymer to have excellent thermal properties, it was necessary to select the appropriate ratio.

Mechanical properties

Tensile properties

Table 4 lists the results of tensile strength and elongation-at-break. The graph is drawn as shown in Figure 10(a), and the stress-strain curves are shown in Figure 9(b). As shown in Figure 10, as the ratio of monomer to catalyst enlarged, the tensile strength and modulus of the polymer showed a downward trend. This was because the active sites participating in the reaction and the crosslink density of the polymer decreased with the reduction of the catalyst. The mechanical properties of non-crystalline polymers such as elasticity and modulus are related to molecular weight and crosslink

Table 3. Mechanical properties data of DMA for PDCPD.

$n_{\text{DCPD}}:n_{\text{Cat}}$	T_g (°C)	E' at 30°C (MPa)	E' at $T_g + 30^\circ\text{C}$ (MPa)	V_c (mol/m ³)
5000:1	151.8	1641.5	47.1	4150.1
10000:1	147.6	1631.5	28.5	2535.8
15000:1	140.7	1626.5	27.0	2439.8
20000:1	130.4	1611.5	16.6	1534.3
30000:1	123.2	1606.5	12.6	1181.9
50000:1	112.3	1492.5	10.9	1053.8

density. An increment in the monomer/catalyst ratio would result in a higher molecular weight and a lower crosslink density. For cross-linked polymers, the mechanical properties were mainly influenced by the crosslink density, provided that the molecular weight was not below a certain value [35]. In the range of this system, the monomer/catalyst ratio grew, the crosslink density (Table 3) and tensile strength of PDCPD became smaller, and its elasticity (the greater elongation-at-break) became better. This was consistent with the trend reported in Ref [9].

When the molar ratio of monomer to catalyst was from 5000:1 to 10000:1, the tensile properties of PDCPD did not change greatly. With decreasing cross-linking density, the active space of polymer became larger under the action of external force, and the elongation rate increased macroscopically. But when the ratio exceeded 10000:1, the tensile properties of PDCPD

became worse. However, the elongation-at-break of the polymer enhanced significantly. By reducing the cross-linking density, the active space of polymer became larger under the action of external force, and the elongation rate increased macroscopically.

Bending performance

The bending performance data of PDCPD under different monomer to catalyst ratios are shown in Figure 10(c). The active sites participating in the reaction and the crosslinking density of the polymer all reduced, resulting in a lower bending strength and modulus of the polymer thanked to the increase in the ratio of monomer to catalyst. Besides, the same as the tensile properties of polymers, 10000:1 was also a turning point in the decline of PDCPD bending performance. When the molar ratio of monomer to catalyst was greater than 10000:1, the bending performance of PDCPD

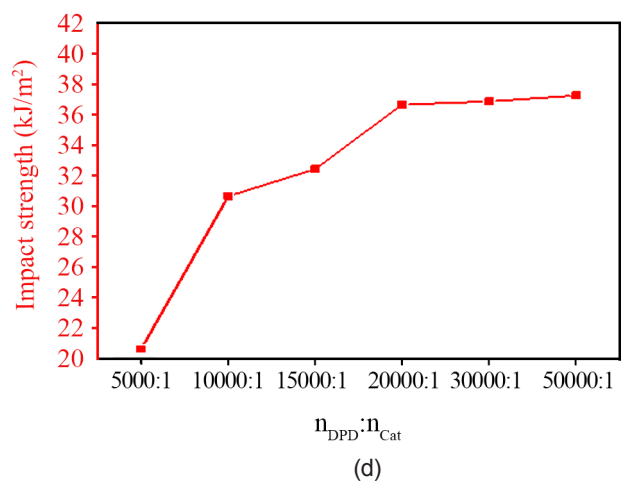
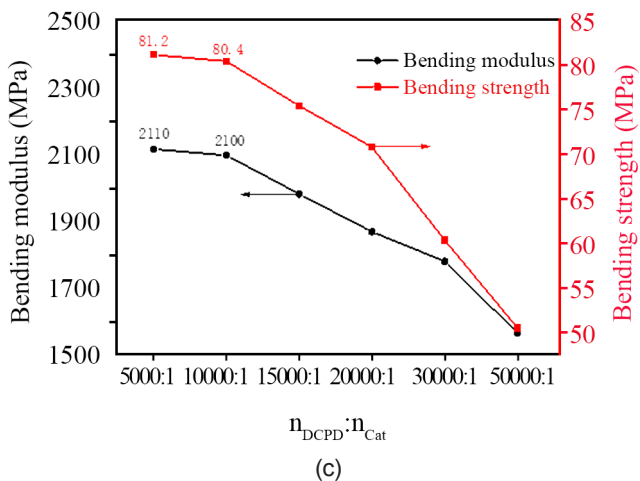
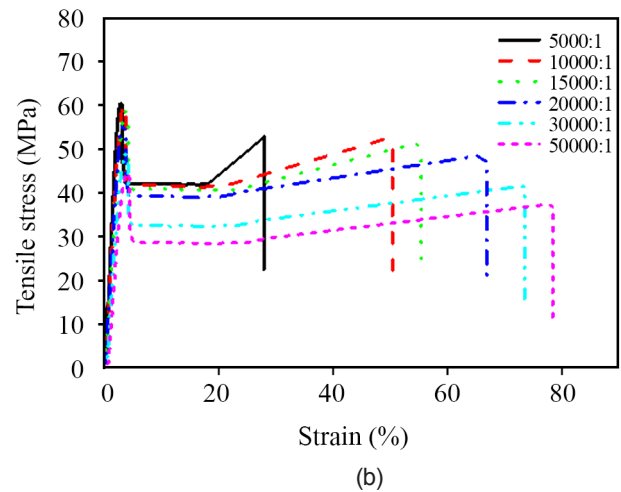
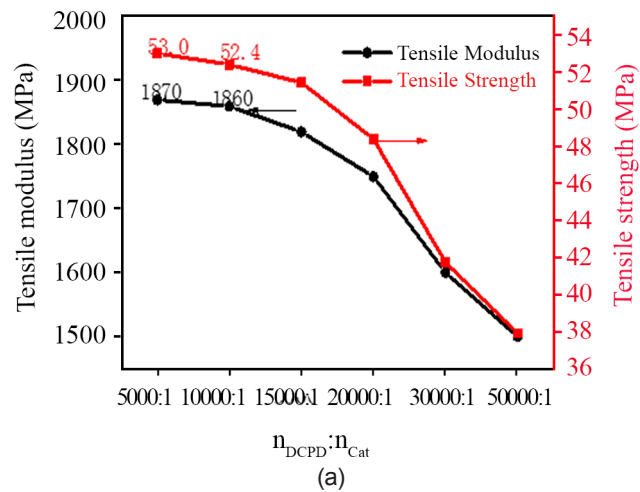


Figure 10. Mechanical properties of PDCPD at different ratios of monomer to catalyst.

deteriorated rapidly. Therefore, the molar ratio of monomer to catalyst should not be too large.

Impact strength

The impact strength of PDCPD at different monomer to catalyst ratios is shown in Figure 10(d). As the ratio of monomer to catalyst increased, the impact strength of the polymer was getting better. This was because the impact toughness at the macroscopic level improved as the catalyst content decreased, resulting in lower crosslinking densities and a larger active PDCPD space. As clearly seen, the strength enhanced by 50% when the amount ratio of monomer to catalyst species was changed from 5000:1 to 10000:1. After that, the growth rate gradually weakened, especially when the ratio of monomer to catalyst material reached 20000:1, the impact strength of PDCPD basically did not change. Therefore, the ratio of monomer to catalyst substance should not be too small, otherwise the impact toughness of the polymer product would be affected.

In summary, the ratio of monomer to catalyst should not be too large, otherwise the tensile and bending properties of the polymer product would be reduced; the ratio of monomer to catalyst should not be too small, which would result in insufficient impact toughness of the polymer. When the molar ratio of monomer and catalyst was 10000:1, PDCPD had the best comprehensive mechanical properties. Its tensile strength, flexural modulus and impact strength reached 52.4 MPa, 2100 MPa and 30 kJ/m², respectively.

At present, the world's leading PDCPD engineering plastics brands include METTON developed by Hercules and Teijin Co., Ltd., and TELENE and PEN-TAM series developed by Goodrich and Zeon Co., Ltd. The properties of PDCPD materials prepared by this process go beyond those of METTON, TELENE and other series of materials.

Thermal stability

To further explore the thermodynamic performance of the materials, the prepared materials were analyzed by thermogravimetric analysis. For the monomer to catalyst of 10000:1, the TGA and DTG spectra of PDCPD are shown in Figure 11. In Figure 11, the weight loss rate of PDCPD at 5%, 10%, 50% and the maximum weight loss rate correspond to the degradation temperatures of

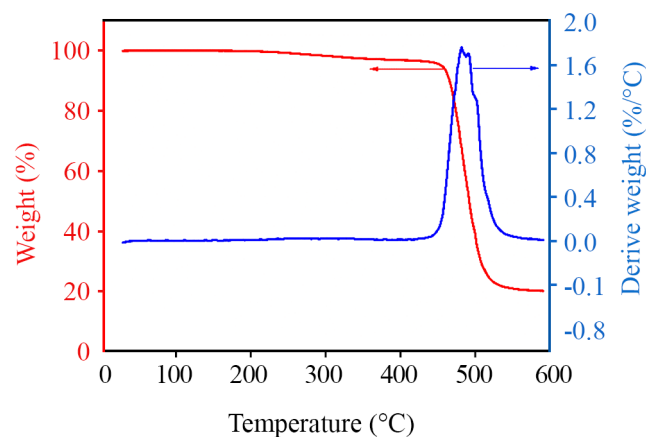


Figure 11. TGA and DTG spectra of PDCPD.

$T_{d5\%}$, $T_{d10\%}$, $T_{d50\%}$ and $T_{d_{max}}$. There was a slight loss of polymer between 250-400°C due to heat loss caused by unreacted DCPD monomer and oligomers formed by small molecules in the system. Subsequently, there was a large weight loss plateau on the thermal weight loss curve of the polymer from 400°C to 500°C, and the polymer degraded rapidly in this range. In summary, the overall thermal stability of PDCPD could reach above 450°C, which is beyond that of many thermo-setting materials.

CONCLUSIONS

In this paper, solution polymerization was firstly carried out in a reagent bottle, and the polymerization process was optimized. Subsequently the formed PDCPD sheet was prepared by using a self-made mold and RIM mechanism, and its polymerization properties and product properties were studied.

The results of curing reaction kinetics showed that the polymerization of DCPD was close to a first-order reaction, and the optimal curing process was divided into two stages: reaction at 60°C for 1 h, followed by post-curing treatment at 140°C for 1 h. The results of polymerization process research showed that the more catalyst content, the higher the reactivity and the shorter the gel curing time. The reaction raw materials could briefly contact with some air during the pretreatment process such as pipetting and mixing, but the reaction mold must be kept in a sealed state. In addition, DCPD could basically be completely converted.

By analyzing the mechanical properties of PDCPD

prepared with different ratios of monomer and catalyst, it was finally determined that the most suitable molar ratio of monomer and catalyst was 10000:1. At this time, the comprehensive mechanical properties of PDCPD reached the best, and its tensile strength, bending strength and impact strength reached 1860 MPa, 2100 MPa and 30 kJ/m², respectively. Besides, PDCPD had good thermal stability. When the ratio of monomer to catalyst material is 10000:1, the overall weight loss temperature of PDCPD can reach above 450°C. The properties of the PDCPD material prepared by this process go beyond those of METTON, TELENE and other series of materials prepared by American and Japanese companies.

CONFLICTS OF INTEREST

The authors declare that they have no conflicts of interest.

REFERENCES

- Kovacic S, Slugovc C (2020) Ring-opening metathesis polymerisation derived poly(dicyclopentadiene) based materials. *Mater Chem Front* 4: 2235-2255
- Jeong W, Kessler MR (2008) Toughness enhancement in ROMP functionalized carbon nanotube/polydicyclopentadiene composites. *Chem Mater* 20: 7060-7068
- Toohey KS, Sottos NR, White SR (2009) characterization of microvascular-based self-healing coatings. *Exp Mech* 49: 707-717
- Hu F, Jie D, Tao O, Zheng Y (2014) Preparation and properties of high performance phthalide-containing bismaleimide reinforced polydicyclopentadiene. *J Appl Polym Sci* 131: 40474-40480
- Martina AD, Hilborn JG, Mühlebach A (2000) Macroporous cross-linked poly(dicyclopentadiene). *Macromolecules* 33: 2916-2921
- Kim HG, Son HJ, Lee DK, Kim DW, Park HJ, Cho DH (2017) Optimization and analysis of reaction injection molding of polydicyclopentadiene using response surface methodology. *Korean J Chem Eng* 34: 2099-2109
- Hu YH, Lang AW, Li XC, Nutt SR (2014) Hygrothermal aging effects on fatigue of glass fiber/polydicyclopentadiene composites. *Polym Degrad Stabil* 110: 464-472
- Mol JC (2004) Industrial applications of olefin metathesis. *J Mol Catal A- Chem* 213: 39-45
- Yao Z, Zhou LW, Dai BB, Cao K (2012) Ring-opening metathesis copolymerization of dicyclopentadiene and cyclopentene through reaction injection molding process. *J Appl Polym Sci* 125: 2489-2493
- Kim HG, Son HJ, Lee DK, Kim DW, Park HJ, Cho DH (2017) Optimization and analysis of reaction injection molding of polydicyclopentadiene using response surface methodology. *Korean J Chem Eng* 34: 2099-2109
- Steese ND, Barvaliya D, Poole XD, McLemore DE, DiCesare JC, Schanz HJ (2018) Synthesis and thermal properties of linear polydicyclopentadiene via ring-opening metathesis polymerization with a third generation grubbs-type ruthenium-alkylidene complex. *Polym Chem* 56: 359-364
- Wang B, Mireles K, Rock M, Li Y, Thakur VK, Gao D, Kessler MR (2016) Synthesis and preparation of bio-based ROMP thermosets from functionalized renewable isosorbide derivative. *Macromol Chem Phys* 217: 871-879
- Cao K, Fu Q, Zhou L, Yao Z (2012) Reaction injection molding of dicyclopentadiene. *Prog Chem* 24: 1368-1377
- Schaubroeck D, Brughmans S, Vercaemst C, Schaubroeck J, Verpoort F (2006) Verpoort. Qualitative FT-Raman investigation of the ring opening metathesis polymerization of dicyclopentadiene. *J Mol Catal A - Chem* 254: 180-185
- Drozdak R, Nishioka N, Recher G, Verpoort F (2010) Latent olefin metathesis catalysts for polymerization of DCPD. *Macromol Symp* 293: 1-4
- Grubbs RH, Chang S (1998) Recent advances in olefin metathesis and its application in organic synthesis. *Tetrahedron* 54: 4413-4450
- Bielawski CW, Grubbs RH (2000) Highly efficient ring-opening metathesis polymerization

- (ROMP) using new ruthenium catalysts containing N-heterocyclic carbene ligands. *Angew Chem Int Ed* 39: 2903-2906
18. Scholl M, Ding S, Lee CW, Grubbs RH (1999) Synthesis and activity of a new generation of ruthenium-based olefin metathesis catalysts coordinated with 1,3-dimesityl-4,5-dihydroimidazol-2-ylidene ligands. *Org Lett* 1: 953-956
 19. Schrock R, Murdzek J, Bazan G (1990) Synthesis of molybdenum imido alkylidene complexes and Some Reactions Involving Acyclic Olefins. *J Am Chem Soc* 112: 3875-3886
 20. Schrock RR (1999) Olefin metathesis by molybdenum imido alkylidene catalysts. *Tetrahedron* 55: 8141-8153
 21. Schrock R (2002) High Oxidation state multiple metal/carbon bonds. *Chem Rev* 102: 145-180
 22. Schrock RR, Hoveyda AH (2003) Molybdenum and tungsten imido alkylidene complexes as efficient olefin-metathesis catalysts. *Angew Chem Int Ed* 42: 4592-4633
 23. Kuang J, Zheng N, Liu C, Zheng Y (2018) Manipulating the thermal and dynamic mechanical properties of polydicyclopentadiene via tuning the stiffness of the incorporated monomers. *e-Polymers* 19: 355-364
 24. Nguyen SBT, Johnson LK, Grubbs RH (1992) Ring-opening metathesis polymerization (ROMP) of norbornene by a group VIII carbene complex in protic media. *J Am Chem Soc* 114: 3974-3975
 25. Arduengo AJ (1999) Looking for stable carbenes: The difficulty in starting anew. *Acc Chem Res* 32: 913-921
 26. Scholl M, Trnka TM, Morgan JP (1999) Increased ring closing metathesis activity of ruthenium-based olefin metathesis catalysts coordinated with imidazol-2-ylidene ligands. *Tetrahedron Lett* 40: 2247-2250
 27. Vidavsky Y, Navon Y, Ginzburg Y, Gottlieb M, Lemcoff NG (2015) Thermal properties of ruthenium alkylidene-polymerized dicyclopentadiene. *Beilstein J Org Chem* 11: 1469-1474
 28. White SR, Sottos NR, Geubelle PH, Moore JS, Kessler MR, Sriram SR, Brown EN, Viswanathan S (2001) Autonomic healing of polymer composites. *Nature* 409: 794-797
 29. Kessler MR, Sottos NR, White SR (2003) Self-healing structural composite materials. *Compos Part A-Appl S* 34: 743-753
 30. Kessler MR, White SR (2002) Cure kinetics of the ring-opening metathesis polymerization of dicyclopentadiene. *J Polym Sci Pol Chem* 40: 2373-2383
 31. Yang G, Lee JK (2013) Effect of Grubbs' catalysts on cure kinetics of endo-dicyclopentadiene. *Thermochim Acta* 566: 105-111
 32. Xia Y, Larock RC (2010) Castor oil-based thermosets with varied crosslink densities prepared by ring-opening metathesis polymerization (ROMP). *Polymer* 51: 2508-2514
 33. Sun Q, Ma S, Ge Z, Luo Y (2017) Preparation and curing behavior of high-stress solid propellant binder based on polydicyclopentadiene. *High Perform Polym* 29: 931-936
 34. Kissinger HE (1957) Reaction kinetics in differential thermal analysis. *Anal Chem* 29: 1702-1706
 35. Zhao F, Bi W, Zhao S (2011) Influence of crosslink density on mechanical properties of natural rubber vulcanizates. *J Macromol Sci Phys* 50: 1460-1469